ATLAS 実験における荷電ヒッグス粒子の探索

筑波大学大学院　数理物質科学研究科　物理学専攻
博士後期課程3年　永田和樹

2016年　1月19日　CiRfSE workshop

重い荷電ヒッグス粒子探索

- もし、荷電ヒッグス粒子の発見できたら
  → 標準理論を超える物理の存在の証明
  - 例：Minimal Supersymmetric Standard Model (MSSM)
- 重い荷電ヒッグス粒子探索 (200~600 GeV)
- 信号生成過程：$g\bar{b} \rightarrow \bar{t}H^{+} \rightarrow \bar{t}t\bar{b} \rightarrow \bar{b}l^{+}\nu b\bar{q}q\bar{b}$
- 重心系衝突エネルギー8 TeV、積分ルミノシティ20.3 fb^{-1}のデータを使用

下図: 信号生成過程のファインマンダイヤグラム

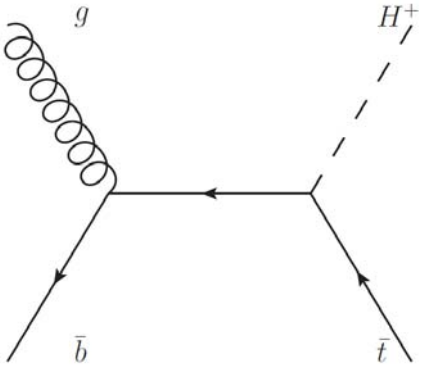

解析の流れ

- 事象選別
  - レプトンやジェットの数、ジェットのフレーバータグ等で、対象とする事象を選別する
- 信号事象と背景事象の分離
  - 信号事象と背景事象の違いを特徴付けるような変数を入力としてMVA(BDT)を行い、S/Bの分離を最適化する
- 生成断面積に対する制限の設定
  - MVAの結果を用いて荷電ヒッグス粒子の生成断面積に対して制限を設定する

事象選別

- 1つのレプトン、4つ以上のジェットを要求
  - レプトン
    - 電子: Pt > 25 GeV, |η| < 2.47
      (1.37 < |η| < 1.52 は除外)
    - ミューオン: Pt > 25 GeV, |η| < 2.5
  - ジェット: Pt > 25 GeV, |η|<2.5
    - b-tag: 70 %の確率でbクォーク由来のジェット(b-jet)を同定

図: ハドロニックH+ 崩壊

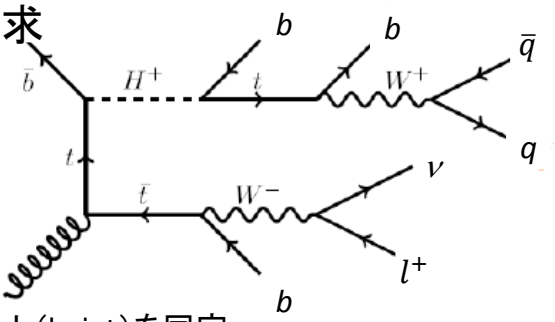

- シグナル領域とコントロール領域に分離
  - シグナル領域: 信号事象を多く含む→ 荷電ヒッグス粒子の探索
  - コントロール領域: ほとんど背景事象→ 背景事象の理解、コントロール

表: 事象中のジェット数とb-tag数に対する2つ領域の定義

	2b-tags	≥ 3b-tags
4jets	コントロール	コントロール
5jets	コントロール	シグナル
>= 6jets	コントロール	シグナル

背景事象の構成要素

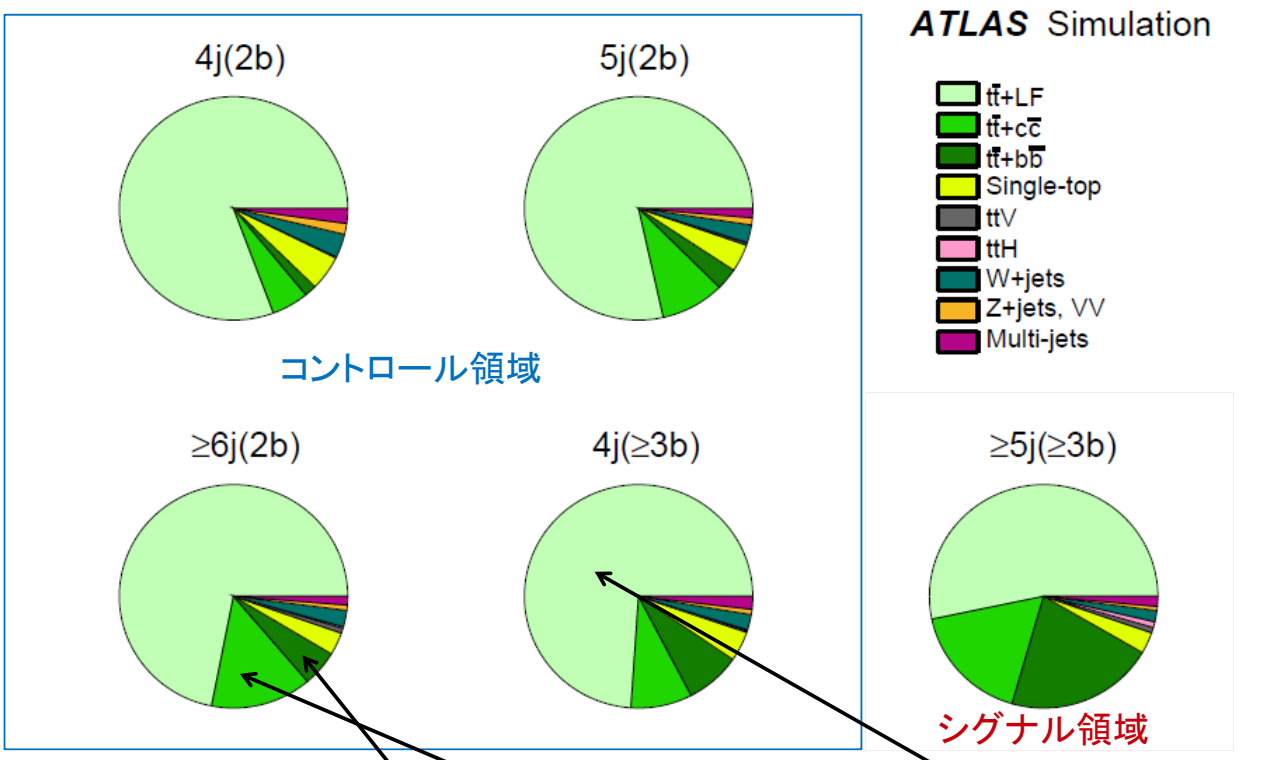

ttbar+Heavy Flavor jets（深緑＋緑）と ttbar+Light Flavor jets（薄緑）が主な背景事象

コントロール領域でのPre-fit plot

- H_T^{had} = ∑ Pt of jets
- 右図： コントロール領域での H_T^{had}の分布
- DataとMCが誤差の範囲で一致している

＊青線、赤線はData数にnormalizeされている

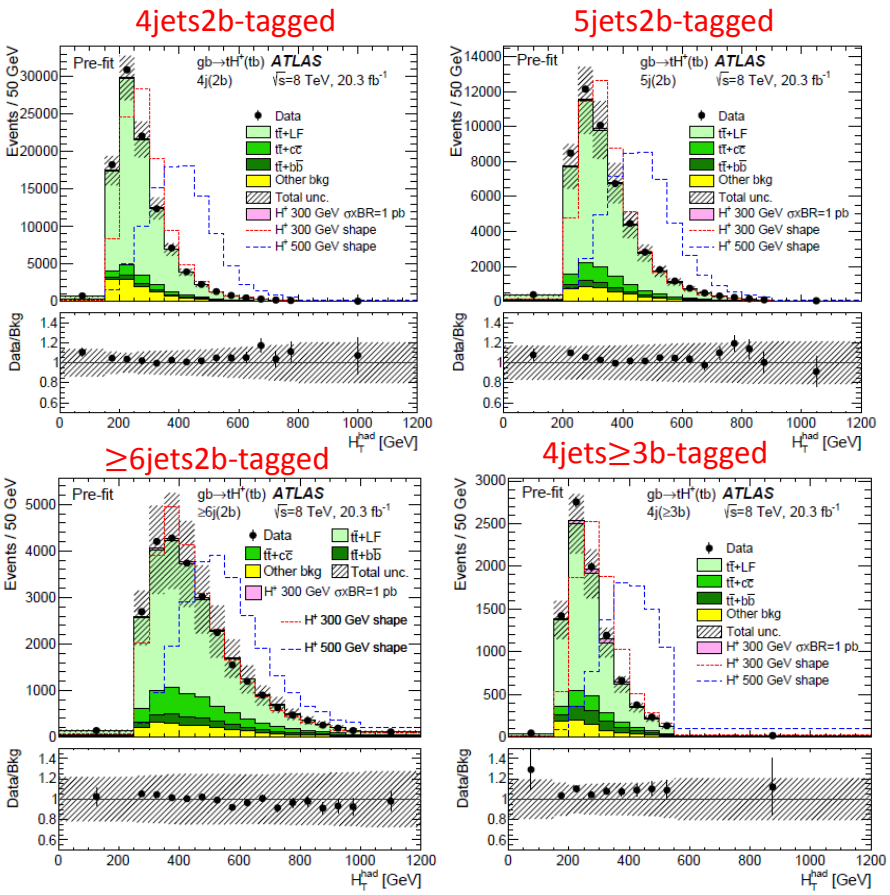

コントロール領域でのPost-fit plot

- 系統誤差も考慮しながら背景事象でフィット
  - 系統誤差の大きさを大幅に減らす
- コントロール領域とシグナル領域で同時にフィット
  - コントロール領域：H_T^{had}
  - シグナル領域：BDT output

DataとMCが誤差の範囲で一致している

4jets2b-tagged

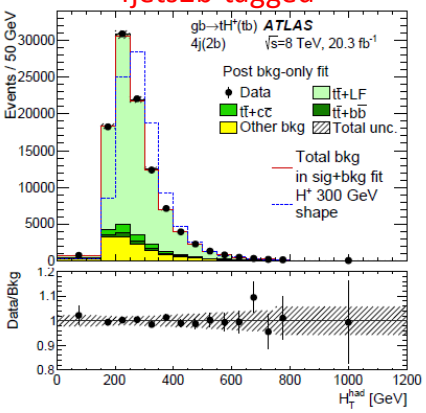

5jets2b-tagged

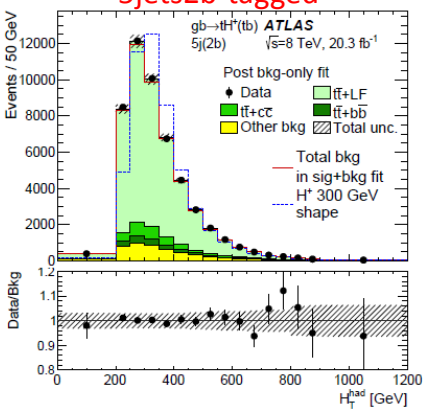

≥6jets2b-tagged

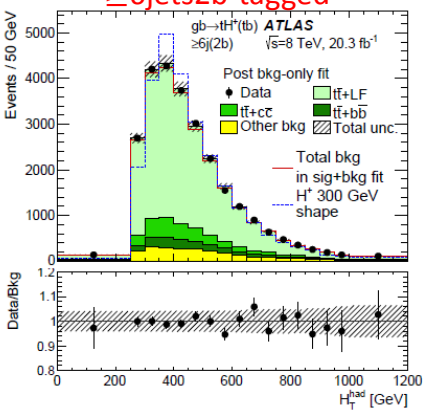

4jets≥3b-tagged

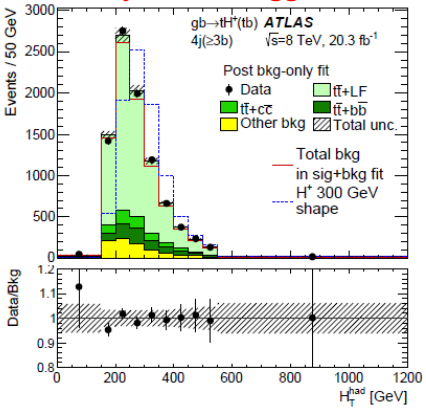

シグナル領域でのBDT outputの分布（post-fit）

$m_{H+} = 300$ GeV

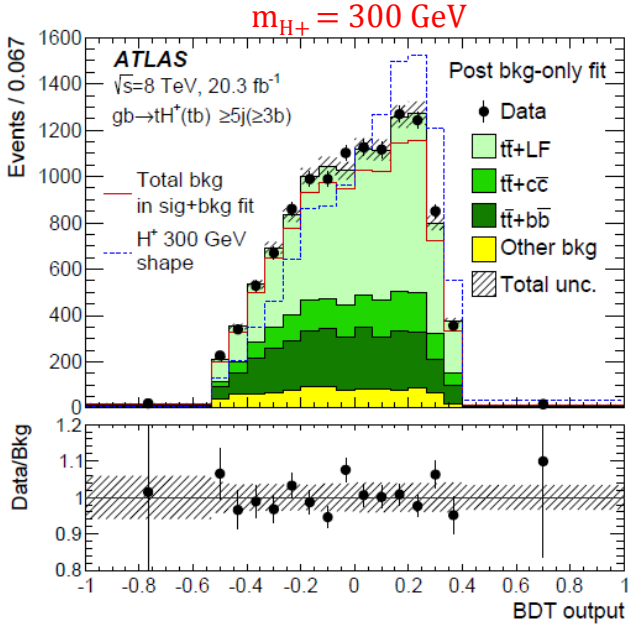

$m_{H+} = 500$ GeV

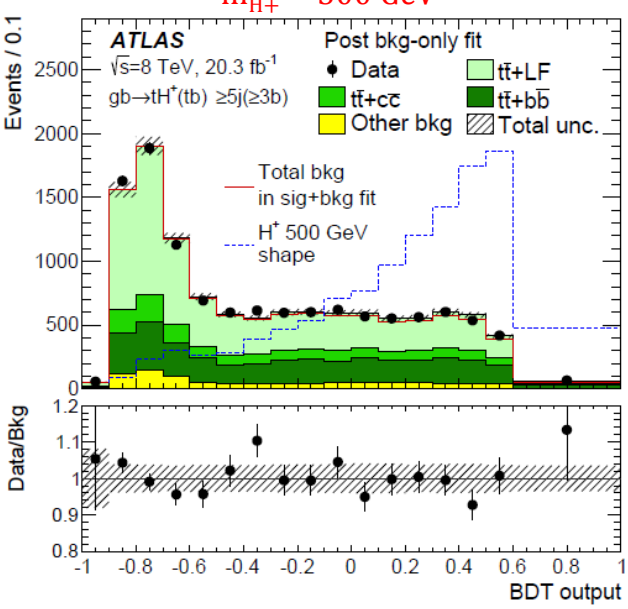

＊青線はData数にnormalizeされている

- High massの方が背景事象と信号事象の分離がよくできる
- $m_{H+} = 300$ GeVにおいて、Signal+background fitの結果とDataの分布が一致しない

生成断面積に対する制限の設定

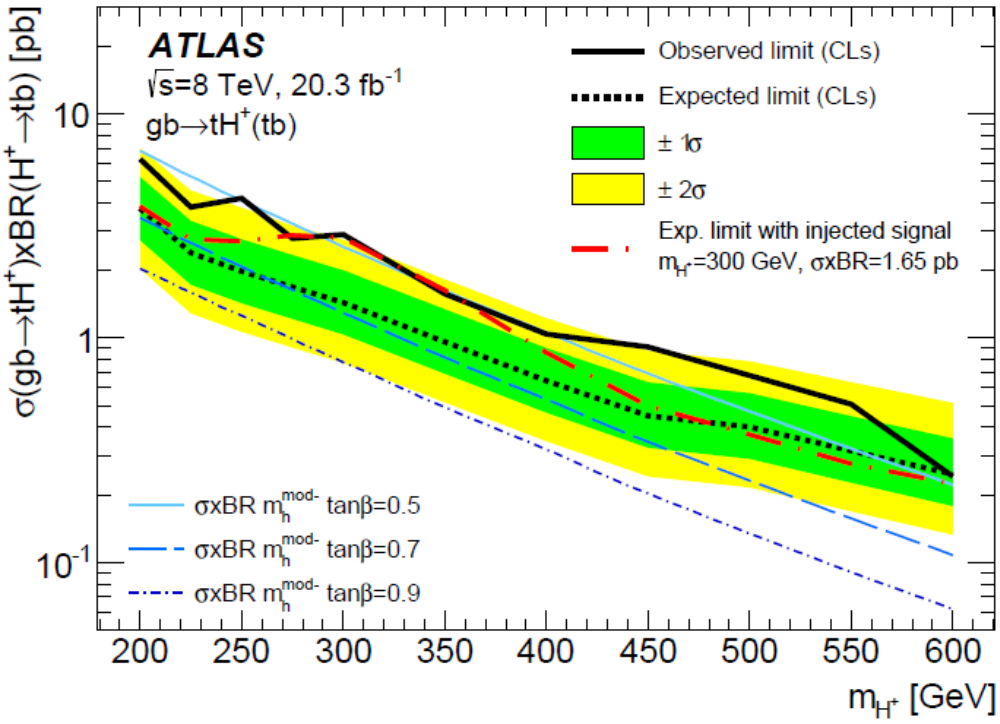

Run1解析の公表

- 最終結果は$H^{\pm} \to tb$のs channelでの解析と合わせる形で出した
- JHEPに論文を2015/12/11にsubmit
  - リンク先： http://inspirehep.net/record/1409300
- 今はAccept待ち

https://twiki.cern.ch/twiki/bin/view/AtlasPublic/HiggsPublicResults

Previous results

New ATLAS/CMS Higgs Couplings Combination

Web page and conference note: ATLAS-CONF-2015-044

Higgs Group Publications

Full Title	Journal	Links	Status	Groups
Search for charged Higgs bosons in the $H^{\pm} → tb$ decay channel in pp collisions at $√s = 8$ TeV using the ATLAS detector	JHEP	Inspire, arXiv, Figures	Submitted: 2015/12/11	HIGGS
Search for the Standard Model Higgs boson produced in association with a vector boson and decaying into a tau pair in pp collisions at $√s\!=\!8\,$TeV with the ATLAS detector	Physical Review D	Figures	Submitted: 2015/11/26	HIGGS
Search for dark matter produced in association with a Higgs boson decaying to two bottom quarks in pp collisions at $√s = 8$ TeV with the ATLAS detector	PRD	Inspire, arXiv, Figures	Submitted: 2015/10/21	EXOT / HIGG
PUBLISHED Search for flavour-changing neutral current top quark decays $t\to Hq$ in pp collisions at $\sqrt{s}=8$ TeV with the ATLAS detector	JHEP	Inspire, arXiv, Figures	JHEP 12 (2015) 061 (Submitted: 2015/09/20)	TOPQ / HIGG

まとめ

- LHC-ATLAS実験で取得された、重心系衝突エネルギー8 TeV、積分ルミノシティ20.3 fb^{-1}のデータを使ってtbに崩壊する重い荷電ヒッグス粒子探索 を行った（200～600 GeV）
- 600 GeVを除くすべての荷電ヒッグス粒子の質量点において、データの超過が見られた
  - 250、300、450 GeVにおいて2.3～2.4σのexcess
- $m_{H+} = 300$ GeV、$\sigma \times \Gamma = 1.65$pbに対応する信号事象を入れてExpected Limitを計算し、Ovserved Limitと比較した。その結果、Ovserved Limitのexcessは背景事象のmissmodelingが原因である可能性が高い
- MSSMのm_h^{mod-} シナリオ、$\tan\beta = 0.5$に対応するモデルに対して、200～300、350～400 GeVまでの領域を排除した

Back up

Signal and Background Modeling

*Background: common with ttH(bb) group

Background process	Subcomponent	Generator & parton shower	Cross section (in pb)	Normalization
$t\bar{t}$ with at least one lepton l		Powheg & Pythia	137.3	top and $t\bar{t}$ Pt reweighting $t\bar{t}$+HF reweighting
Single top	t-channel (with l)	AcerMC & Pythia	28.4	Theoretical cross section
	s-channel (with l)	Powheg & Pythia	1.8	
	Wt-channel	Powheg & Pythia	22.4	
W + jets	$W(l\nu)$+jets	Alpgen & Pythia	3.6×10^4	W Pt reweighting
	$Wb\bar{b}$ + jets		1.5	
	$Wc\bar{c}$ + jets		4.8	
	W + c + jets		1.7	
Z + jets	$Z/\gamma^*(ll)$+jets, $m(ll) > 60$ GeV	Alpgen & Pythia	3.4×10^3	Z Pt reweighting
	$Z/\gamma^*(ll)b\bar{b}$+jets, $m(ll) > 30$ GeV		41.3	
	$Z/\gamma^*(ll)c\bar{c}$+jets, $m(ll) > 30$ GeV		84.8	
Diboson	WW	Alpgen & Herwig	29.7	Theoretical cross section
	ZZ		1.5	
	WZ		2.3	
	WZ(with one l)	Sherpa	6.01	
$t\bar{t}$ + V		MadGraph & Pythia	0.44	Theoretical cross section
$t\bar{t}H(m_H = 125$ GeV)	Semilepton	Powhel & Pythia	0.0566	Theoretical cross section
$t\bar{t}H(m_H = 125$ GeV)	Dilepton		0.0136	
Misidentified lepton				Data
$H^+(m_{H^+} = 180 \sim 600$ GeV)	Semilepton	Powheg & Pythia	1.0	Theoretical cross section
$H^+(m_{H^+} = 180 \sim 600$ GeV)	Dilepton		1.0	

Analysis Outline

- Event selection
  - Based on standard top group selection: 1 lepton, > 3jets, MET
    - 1lepton trigger:
      - EF e24vhi medium1 or EF e60 medium1
      - EF mu24i tight or EF mu36 tight
    - Electron: Author 1 or 3, Tight, Pt > 25 GeV, $|\eta| < 2.47$ ($1.37 < |\eta| < 1.52$ excluded), $z_0 <$ 2mm, p_T and $|\eta|$ dependent tracking isolation (corresponding to 90% signal efficiency)
    - Muon: Combined and Tight, Pt > 25 GeV, $|\eta| < 2.47$, $z_0 <$ 2mm, Track isolation using p_T dependent cone, $\Sigma p_T < 0.05 * p_T$
    - Jets: Anti-kt 0.4, LCW, pt > 25 GeV, $|\eta| < 2.5$, Jet vertex fraction cut: $|JVF| > 0.5$ for pT < 50 GeV and $|\eta| < 2.4$
    - B-tag: MV1, working point= 70% efficiency for b-jets in tt events
    - MET: MET AntiKt4LCTopoJets tightpp
  - Separate signal and control regions
    - Signal region: >= 5jets and >= 3b-tags
    - Control region: ==4jets and >= 2b-tags, >= 5jets and == 2b-tags
- S/B separation
- Limit setting

Pre-fit event yield table for background

Process	4j(2b)	5j(2b)	≥6j(2b)	4j(≥3b)	≥5j(≥3b)
$t\bar{t}$+LF	80 300 ± 9 900	38 700 ± 7 400	19 300 ± 5 300	6 300 ± 1 000	5 600 ± 1 600
$t\bar{t}$+$c\bar{c}$	5 200 ± 2 900	4 500 ± 2 600	3 800 ± 2 300	740 ± 410	1 800 ± 1 000
$t\bar{t}$+$b\bar{b}$	1 720 ± 940	1 550 ± 830	1 390 ± 820	660 ± 370	2 300 ± 1 200
$t\bar{t}H$	33.7 ± 4.6	44.6 ± 5.4	68.9 ± 9.1	15.5 ± 2.5	87 ± 11
$t\bar{t}V$	128 ± 40	151 ± 47	189 ± 59	17.6 ± 5.7	85 ± 27
Single-top	5 020 ± 770	1 970 ± 420	880 ± 270	360 ± 83	330 ± 110
W+jets	3 400 ± 1 700	1 270 ± 720	640 ± 400	190 ± 100	170 ± 100
Z+jets	1 330 ± 670	400 ± 220	150 ± 95	53 ± 31	49 ± 39
VV	232 ± 69	108 ± 41	52 ± 25	10.7 ± 3.6	13.7 ± 6.0
Multi-jets	2 160 ± 870	670 ± 260	330 ± 150	160 ± 67	150 ± 100
Total bkg	100 000 ± 11 000	49 300 ± 8 600	27 100 ± 6 600	8 500 ± 1 300	10 600 ± 2 500
Data	102 462	51 421	26 948	9 102	11 945

Table 1: Expected event yields of the SM background processes and observed data in the five categories. The first four columns show the event yields in the CR, the last column shows the event yields in the SR. The uncertainties include statistical and systematic components (systematic uncertainties are discussed in section 4.3).

Pre-fit event yield table for signal (MSSM m_{hmod-})

m_{H^+} [GeV]	$\tan\beta$	4j(2b)	5j(2b)	≥6j(2b)	4j(≥3b)	≥5j(≥3b)
200	0.5	2 580 ± 420	1 670 ± 190	1 050 ± 300	730 ± 190	1 750 ± 200
	0.7	1 290 ± 210	834 ± 93	520 ± 150	366 ± 95	880 ± 100
	0.9	760 ± 120	493 ± 55	309 ± 88	216 ± 56	518 ± 59
400	0.5	397 ± 69	406 ± 44	390 ± 100	211 ± 56	756 ± 76
	0.7	200 ± 35	204 ± 22	197 ± 51	106 ± 28	380 ± 38
	0.9	119 ± 21	121 ± 13	117 ± 31	63 ± 17	226 ± 23
600	0.5	71 ± 14	85 ± 12	107 ± 29	36 ± 11	183 ± 23
	0.7	34.7 ± 6.9	41.5 ± 5.6	52 ± 14	17.4 ± 5.3	89 ± 11
	0.9	19.8 ± 3.9	23.7 ± 3.2	29.8 ± 8.1	10.0 ± 3.0	50.9 ± 6.5

Table 2: Number of expected signal events in the five categories for a few representative points of the $m_h^{\text{mod}-}$ scenario of the MSSM. The last column shows the event yields in the SR. The expected uncertainties contain statistical and systematic components (systematic uncertainties are discussed in section 4.3). Uncertainties on the cross sections and branching fractions for the $m_h^{\text{mod}-}$ scenario are not included.

BDT input variables for training

- The scalar sum of the P_T of all selected jets
- The pT of the leading jet
- The invariant mass of the two b-tagged jets that are closest in ΔR
- The second Fox–Wolfram moment, calculated from the selected jets
- The average ΔR between all pairs of b-tagged jets in the event

＊それぞれの荷電ヒッグスのmass pointごとにトレーニングをおこなった

Fox-Wolfram Moments（H+ analysis）

- Fox-Wolfram moments , W_l(l = 0, 1, 2, …)
- $W_l = \sum_{i,j=0}^{N} \frac{|\overrightarrow{p_i}||\overrightarrow{p_j}|}{E^2} P_l(\cos\Omega_{ij})$

Pi,j= ジェットの運動量
E= イベント中のジェットのエネルギーの和
$P_l(\cos\Omega_{ij})$ = ルジャンドル多項式
$\cos\Omega_{ij}$ = cosθi cosθj + sinθi sinθj cos(ϕi-ϕj)

Pre-fit plots in signal region (part1)

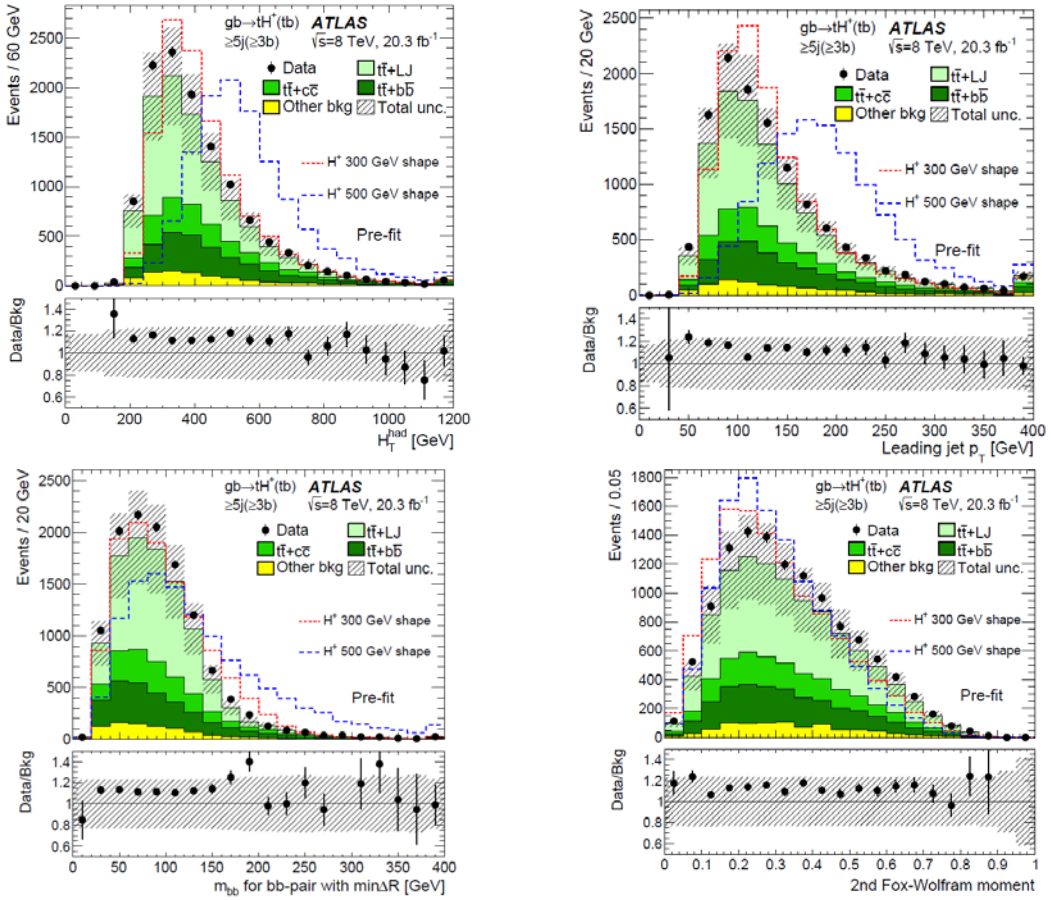

Pre-fit plots in signal region (part2)

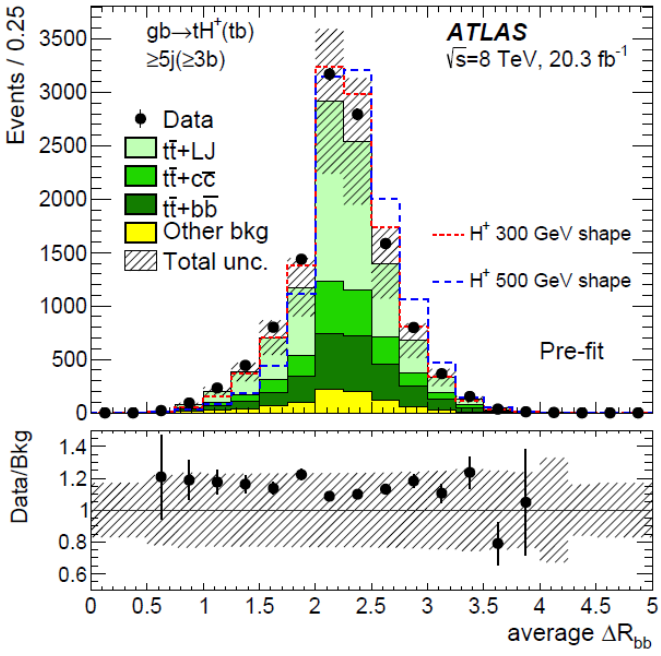

Pre-fit plot for BDT output in control region

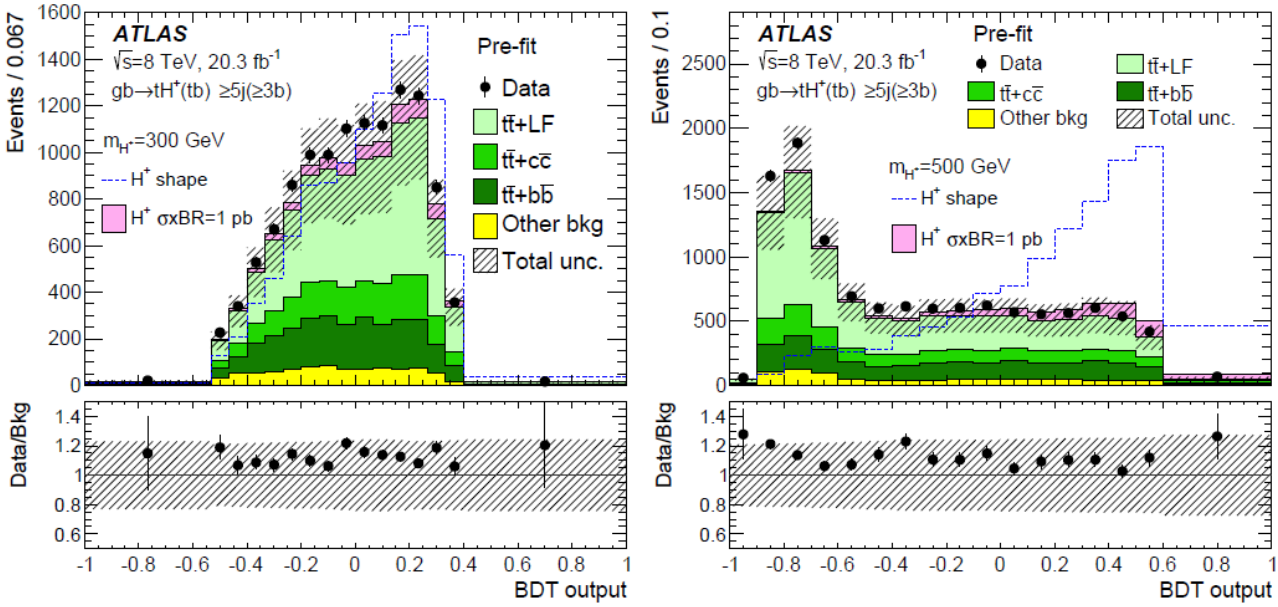

＊青線はData数にnormalizeされている

High massの方が信号事象と背景事象の分離が良い

Systematic uncertainty 一覧

- Type
  - N: normalizationに影響
  - S：sharpeに影響

Systematic uncertainty	Type	Components
Luminosity	N	1
Reconstructed objects		
Electron	SN	5
Muon	SN	6
Jet energy scale	SN	22
Jet energy resolution	SN	1
Jet vertex fraction	SN	1
Jet reconstruction efficiency	SN	1
b-tagging efficiency	SN	6
c-tagging efficiency	SN	4
LF-tagging efficiency	SN	12
High-p_{T} b-tagging efficiency	SN	1
Background modelling		
$t\bar{t}$ cross section	N	1
$t\bar{t}$ modelling: parton shower	SN	3
$t\bar{t}$ modelling: p_{T} reweighting	SN	9
$t\bar{t}$+HF: normalisation	N	2
$t\bar{t}+c\bar{c}$: p_{T} reweighting	SN	2
$t\bar{t}+c\bar{c}$: generator	SN	4
$t\bar{t}+b\bar{b}$: NLO shape	SN	8
Single-top-quark cross section	N	1
Single-top-quark model	SN	1
$t\bar{t}V$ cross section	N	1
$t\bar{t}V$ model	SN	1
W+jets normalisation	N	3
W p_{T} reweighting	SN	1
Z+jets normalisation	N	3
Z p_{T} reweighting	SN	1
Diboson normalisation	N	3
Multi-jets: normalisation	N	2
Multi-jets: method	SN	3
Signal modelling		
$H^+ \to tb$: generator	N	1
$H^+ \to tb$: scales	N	1
$H^+ \to tb$: PDF	SN	1

Systematic uncertainty

Source of uncertainty	Fractional uncertainty [%]	
	m_{H^+} = 300 GeV	m_{H^+} = 500 GeV
$t\bar{t}$ modelling	31	33
Jets	21	9.5
Flavour tagging	19	24
Other background modelling	9.6	12
Signal modelling	8.0	3.5
Lepton	1.2	0
Luminosity	1.1	0.4
Statistics	8.9	18

Table 3: Fractional uncertainty on the parameter of interest relative to its total uncertainty, broken down into various sources and for two mass hypotheses. The values are obtained after fits to the background-plus-signal hypothesis. The largest contribution to the total uncertainty comes from the $t\bar{t}$ modelling.

Symmetrised pre-fit uncertainties in %

Uncertainty	$t\bar{t}$+$b\bar{b}$	$t\bar{t}$+$c\bar{c}$	$t\bar{t}$+LF	$t\bar{t}H$	$t\bar{t}V$	Single-top	W+jets	Z+jets	VV	Multi-jets	H^+
Cross section	50	50	5.5	11	30	4.5	54	54	34	-	-
Luminosity	2.8	2.8	2.8	2.8	2.8	2.8	2.8	2.8	2.8	-	2.8
Light jet rej.	0.68	2.0	4.7	0.61	1.9	4.5	13	18	5.5	-	0.76
b-tagging	6.6	4.8	5.2	5.7	5.5	5.8	4.5	4.5	6.6	-	6.1
c-tagging	0.92	6.9	5.5	1.3	4.1	4.9	5.7	3.1	4.8	-	0.68
Jet sys.	5.1	6.7	8.6	3.4	3.8	12	16	45	21	-	4.3
Lepton sys.	1.5	1.5	1.5	1.5	0.06	1.6	1.7	2.1	1.7	-	1.5
$t\bar{t}$ reweightings	8.2	13	8.1	-	-	-	-	-	-	-	-
$t\bar{t}$ parton shower	6.3	16	22	-	-	-	-	-	-	-	-
Other bkg model.	-	-	-	-	0.73	17	4.9	4.6	-	67	-
H^+ modelling	-	-	-	-	-	-	-	-	-	-	4.9

Nuisance parameters that have large correlations

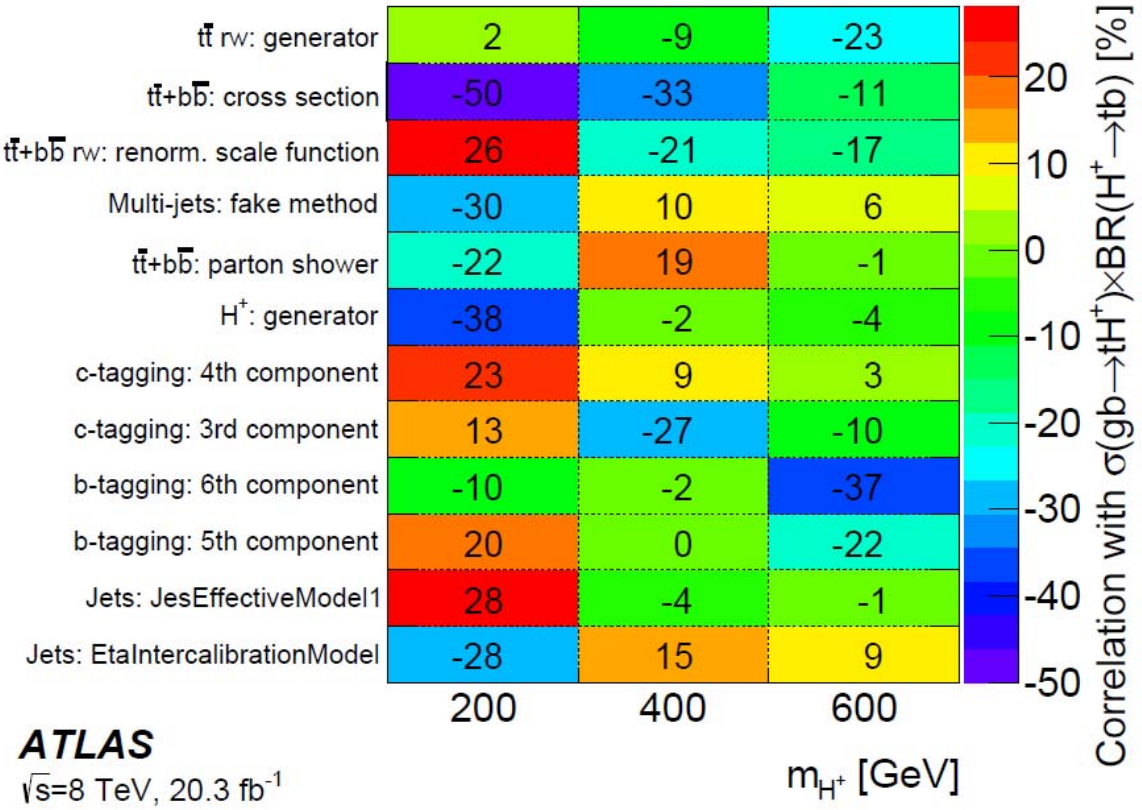

Post-fit pulls and impact of the 15 most relevant uncertainties on the best-fit value

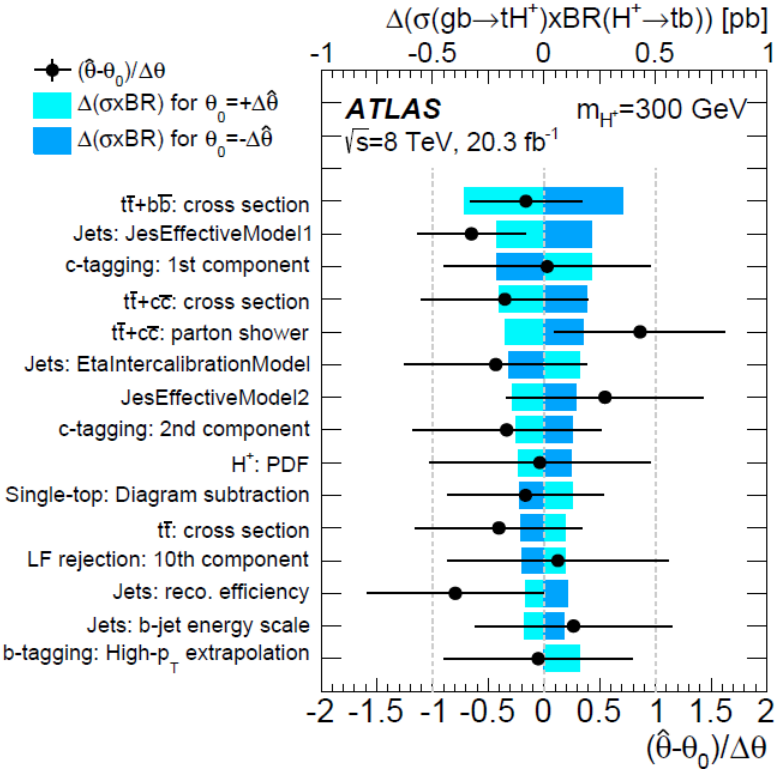

Post-fit pulls and impact of the relevant uncertainties on the best-fit value

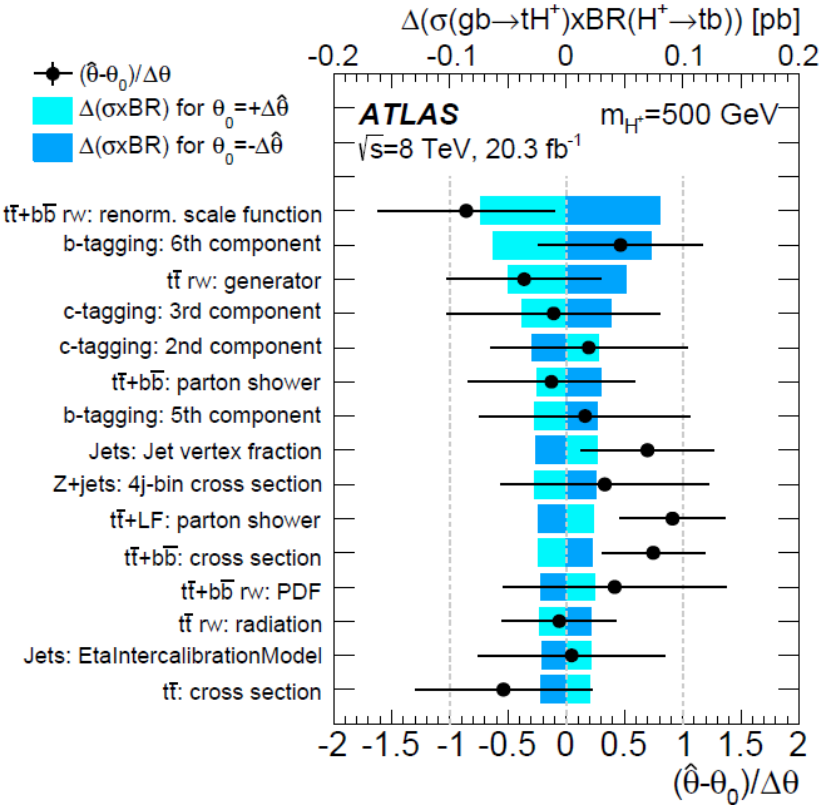

post-fit後の事象数

Process	4j(2b)	5j(2b)	≥6j(2b)	4j(≥3b)	≥5j(≥3b)
$t\bar{t}$+LF	83 600 ± 1 900	41 800 ± 1 400	21 000 ± 1 000	6 750 ± 270	6 650 ± 390
$t\bar{t}$+$c\bar{c}$	3 200 ± 1 700	2 600 ± 1 400	2 100 ± 1 200	490 ± 230	1 260 ± 570
$t\bar{t}$+$b\bar{b}$	1 500 ± 530	1 300 ± 440	1 050 ± 450	600 ± 210	2 040 ± 550
$t\bar{t}H$	34.6 ± 3.8	44.6 ± 4.9	66.7 ± 7.8	16.2 ± 1.9	87 ± 10
$t\bar{t}V$	132 ± 39	153 ± 46	186 ± 57	18.5 ± 5.4	87 ± 26
Single-top	5 030 ± 530	1 970 ± 270	860 ± 170	386 ± 55	342 ± 70
W+jets	4 500 ± 1 100	1 660 ± 470	750 ± 270	250 ± 62	220 ± 69
Z+jets	1 330 ± 560	370 ± 190	137 ± 80	56 ± 23	36 ± 27
VV	223 ± 63	103 ± 39	47 ± 23	10.4 ± 3.1	15.0 ± 5.3
Multi-jets	2 230 ± 590	690 ± 180	330 ± 100	160 ± 46	208 ± 88
Total bkg	101 800 ± 2 200	50 700 ± 1 600	26 600 ± 1 100	8 730 ± 330	10 950 ± 490
H^+	700 ± 310	600 ± 260	430 ± 190	370 ± 160	990 ± 440
Data	102 462	51 421	26 948	9 102	11 945

BDT output distribution in signal region (post background only fit, mH+=200 GeV)

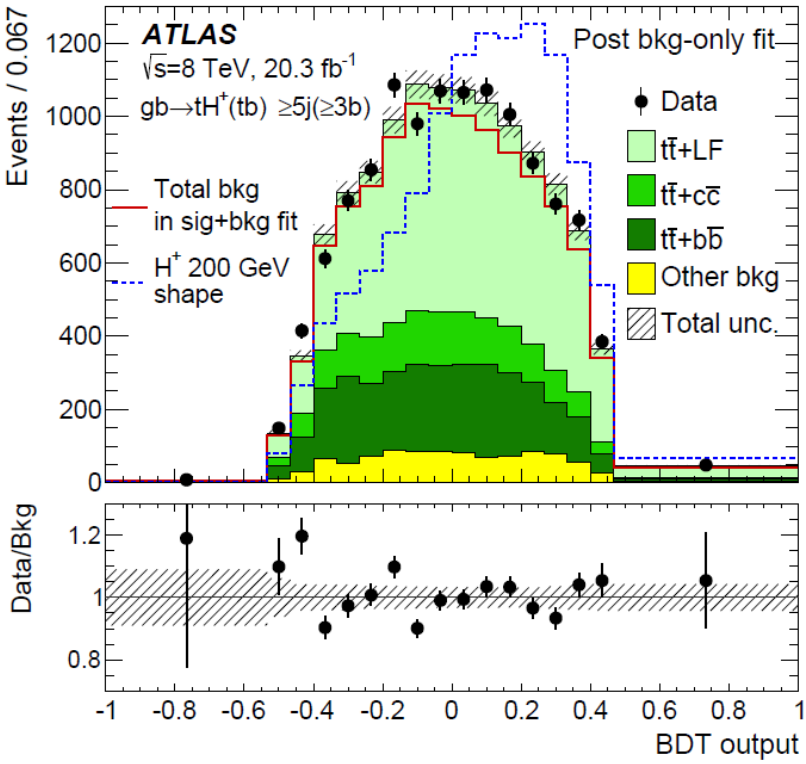

BDT output distribution in signal region (post background only fit, mH+=400 GeV)

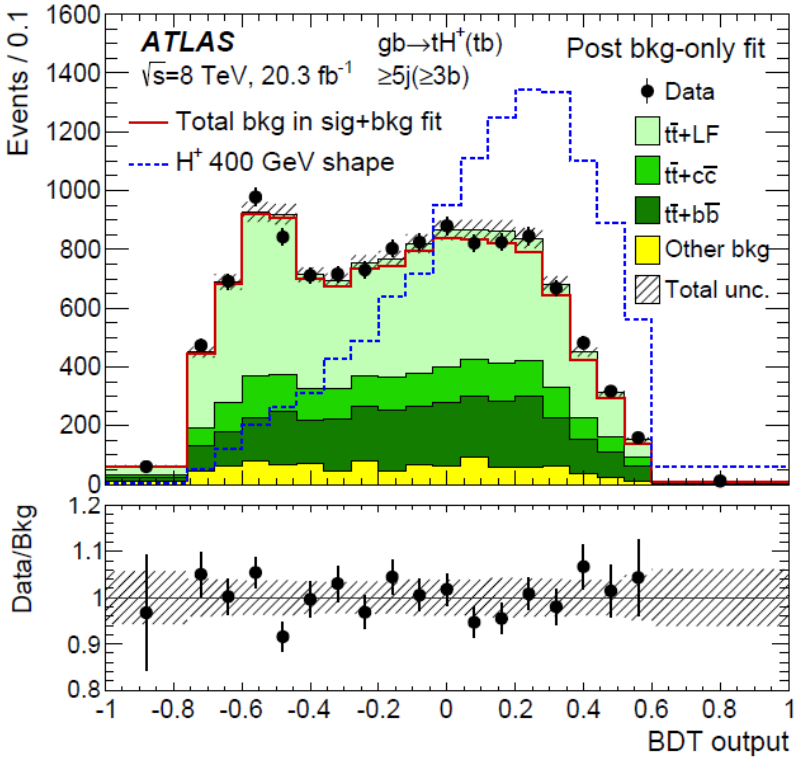

BDT output distribution in signal region (post background only fit, mH+=600 GeV)

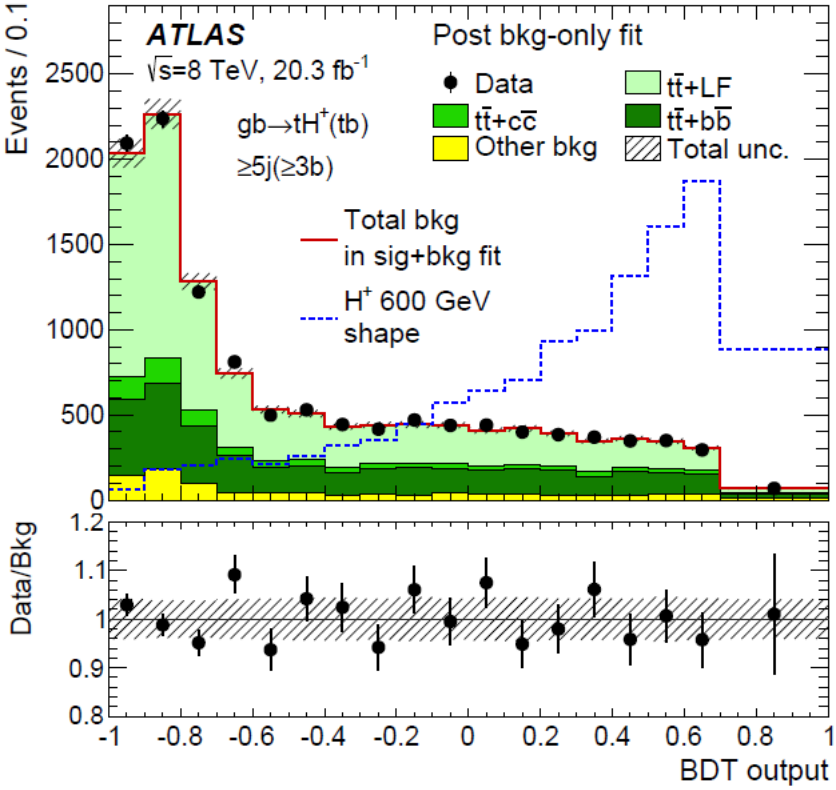

2 Higgs Doublet Model

- Added one Higgs doublet to SM
  - h^0, H^0 (CP even), A^0 (CP odd), $H^{\pm}$(charged)
  - Assume the discovered Higgs = light CP-even Higgs boson, h^0
- 4 Types
  - Different couplings of quarks, leptons and vector bosons to Higgs fields

Table: Coupling scale factor: $k = g^{2HDM}/g^{SM}$ (g^{2HDM}=light Higgs boson coupling)

Coupling scale factor	Type I	Type II	Type III	Type IV
κ_V	$\sin(\beta-\alpha)$	$\sin(\beta-\alpha)$	$\sin(\beta-\alpha)$	$\sin(\beta-\alpha)$
κ_u	$\cos(\alpha)/\sin(\beta)$	$\cos(\alpha)/\sin(\beta)$	$\cos(\alpha)/\sin(\beta)$	$\cos(\alpha)/\sin(\beta)$
κ_d	$\cos(\alpha)/\sin(\beta)$	$-\sin(\alpha)/\cos(\beta)$	$\cos(\alpha)/\sin(\beta)$	$-\sin(\alpha)/\cos(\beta)$
κ_l	$\cos(\alpha)/\sin(\beta)$	$-\sin(\alpha)/\cos(\beta)$	$-\sin(\alpha)/\cos(\beta)$	$\cos(\alpha)/\sin(\beta)$

$\tan\beta=\frac{v2}{v1}$ α: mixing angle of h^0 and H^0 v_1,v_2=vacuum expectation values (plural)

- Different rates of h^0 productions and decays from SM Higgs
- Constrain 2HDM parameters

Stop and Sbottom mass

- Radiative correction to Higgs mass
  - top/stop sector
  - tau/stau and bottom/sbottom sector (high tanβ)
- No mixing: mh ≤ 122 GeV
- mh max: mh ≤ 135 GeV
- mass matrix for $\widetilde{t_R}$, $\widetilde{t_L}$ and $\tilde{b}_R$, $\tilde{b}_L$ eigenstates

$$\mathcal{M}^2_{\tilde{t}} = \begin{pmatrix} M^2_{\tilde{t}_L} + m_t^2 + \cos 2\beta(\frac{1}{2} - \frac{2}{3}s^2_{\rm w})M_Z^2 & m_t X_t^* \\ m_t X_t & M^2_{\tilde{t}_R} + m_t^2 + \frac{2}{3}\cos 2\beta s^2_{\rm w} M_Z^2 \end{pmatrix},$$

$$\mathcal{M}^2_{\tilde{b}} = \begin{pmatrix} M^2_{\tilde{b}_L} + m_b^2 + \cos 2\beta(-\frac{1}{2} + \frac{1}{3}s^2_{\rm w})M_Z^2 & m_b X_b^* \\ m_b X_b & M^2_{\tilde{b}_R} + m_b^2 - \frac{1}{3}\cos 2\beta s^2_{\rm w} M_Z^2 \end{pmatrix},$$

where

$$m_t X_t = m_t(A_t - \mu^* \cot\beta), \quad m_b X_b = m_b(A_b - \mu^* \tan\beta).$$

- At, Ab: trilinear Higgs-stop, sbottom coupling
- μ: Higgsino mass
- s_w: $\sqrt{1 - cw}$, c_w = Mw/Mz

Parameter setting (m_h mod)

– The $m_{\rm h}^{\rm mod}$ scenario:

Departing from the parameter configuration that maximizes $M_{\rm h}$, one naturally finds scenarios where in the decoupling region the value of $M_{\rm h}$ is close to the observed mass of the signal over a wide region of the parameter space. A convenient way of modifying the $m_{\rm h}^{\rm max}$ scenario in this way is to reduce the amount of mixing in the stop sector, i.e. to reduce $|X_{\rm t}/M_{\rm SUSY}|$ compared to the value of ≈ 2 (FD calculation) that gives rise to the largest positive contribution to $M_{\rm h}$ from the radiative corrections. This can be done for both signs of $X_{\rm t}$.

$$\begin{aligned} m_{\rm h}^{\rm mod+}: \quad & M_{\rm SUSY} = 1000\ {\rm GeV}, \mu = 200\ {\rm GeV}, M_2 = 200\ {\rm GeV}, \\ & X_{\rm t}^{\rm OS} = 1.5\, M_{\rm SUSY}\ ({\rm FD\ calculation}), X_{\rm t}^{\overline{\rm MS}} = 1.6\, M_{\rm SUSY}\ ({\rm RG\ calculation}), \\ & A_{\rm b} = A_\tau = A_{\rm t}, M_{\tilde{\rm g}} = 1500\ {\rm GeV}, M_{\tilde{\rm l}_3} = 1000\ {\rm GeV}\ . \end{aligned} \tag{362}$$

$$\begin{aligned} m_{\rm h}^{\rm mod-}: \quad & M_{\rm SUSY} = 1000\ {\rm GeV}, \mu = 200\ {\rm GeV}, M_2 = 200\ {\rm GeV}, \\ & X_{\rm t}^{\rm OS} = -1.9\, M_{\rm SUSY}\ ({\rm FD\ calculation}), X_{\rm t}^{\overline{\rm MS}} = -2.2\, M_{\rm SUSY}\ ({\rm RG\ calculation}), \\ & A_{\rm b} = A_\tau = A_{\rm t}, M_{\tilde{\rm g}} = 1500\ {\rm GeV}, M_{\tilde{\rm l}_3} = 1000\ {\rm GeV}\ . \end{aligned} \tag{363}$$

MSSM Higgs Decay

- A MSSM Higgs decay mode
  - ➢ The Higgs mass
  - ➢ tanβ
  - ➢ Scenario: Changing parameters related with SUSY
    - mh max: h0 mass is maximized for fixed tanβ, mA (h0 < 135 GeV)
    - mh mod±: modification of mh max(±: sign of $|X_t/M_{SUSY}|$)

*Requirement of 2HDM: Triangle anomalies from higgsino is canceled by introducing additional Higgs doublet

H^+ Decay mode for m_h max scenario

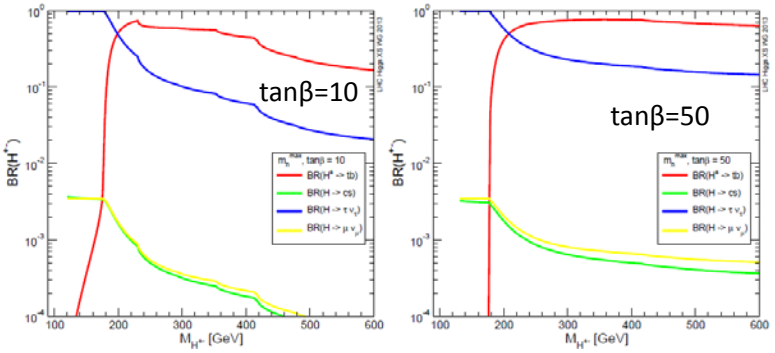

H^+ Decay mode for mh mod- scenario

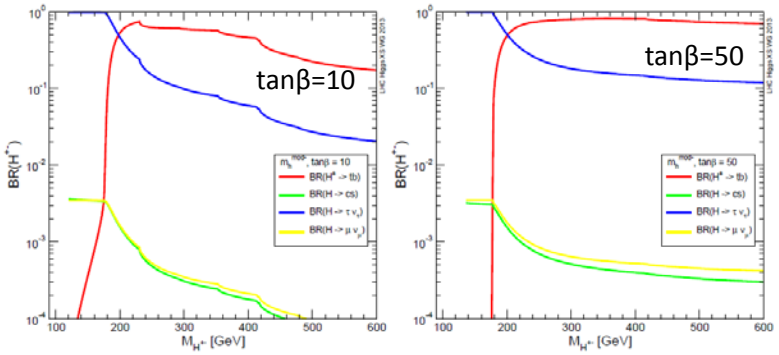

Direct search: MSSM $H^{\pm} \rightarrow \tau^{\pm}\nu$

ATLAS-CONF-2014-050

- Production process
  - $mH^{\pm} < m_{top}$: gluon fusion
    - Top quark decay
  - $mH^{\pm} > m_{top}$: With top quark (hadronic decay)
    - Cross section: Evaluated on 4Flavor Scheme and 5 Flavor Scheme
- $H^{\pm} \rightarrow \tau^{\pm}\nu$ decay
  - $mH^{\pm} < m_{top}$: dominant decay
  - $mH^{\pm} > m_{top}$: second dominant decay
    - ~1/5 × Br($H^{\pm} \rightarrow tb$) in high tanβ

$H^{\pm}$ Decay mode for m_h max scenario

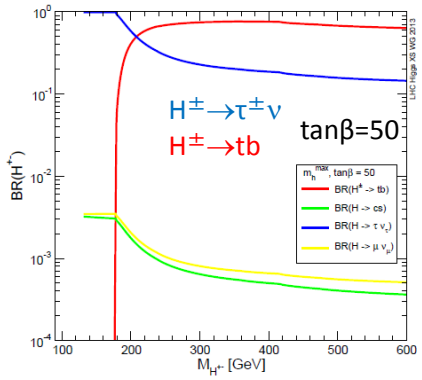

*m_h max scenario is explained at page 12

gluon fusion

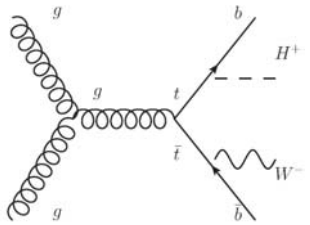

Same process, but different calculation for x-sec

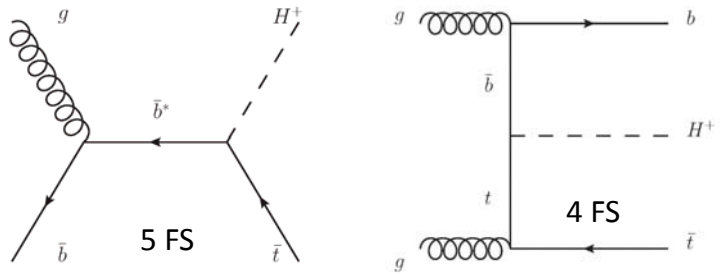

4FS and 5FS

- 4FS and 5FS: Different way of ordering perturbation theory
- 4FS (gg → bbarH)
  - mb >> QCD scale, calculated order by order
  - not b-quarks as partons in the proton
- 5FS (gg → (bbar)H
  - logarithms of the form ln(μF/mb) in gluon splitting, μF ≈ mH/4
  - 4FS: Collinearly b-quarks and H >> 4mb, ln(μF/mb) -> ∞
  - 5FS: ln(μF/mb) terms can be summed to all orders in perturbation theory by introducing bottom parton densities

4 FS

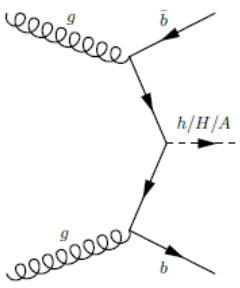

5 FS

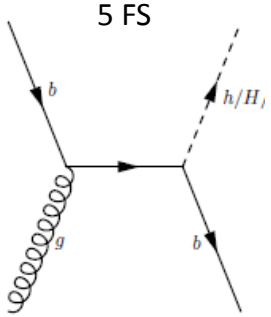

Santander matching

$$\sigma^{\text{matched}} = \frac{\sigma^{4\text{FS}} + w\,\sigma^{5\text{FS}}}{1+w} \qquad w = \ln\frac{m_{\text{H}}}{m_{\text{b}}} - 2$$

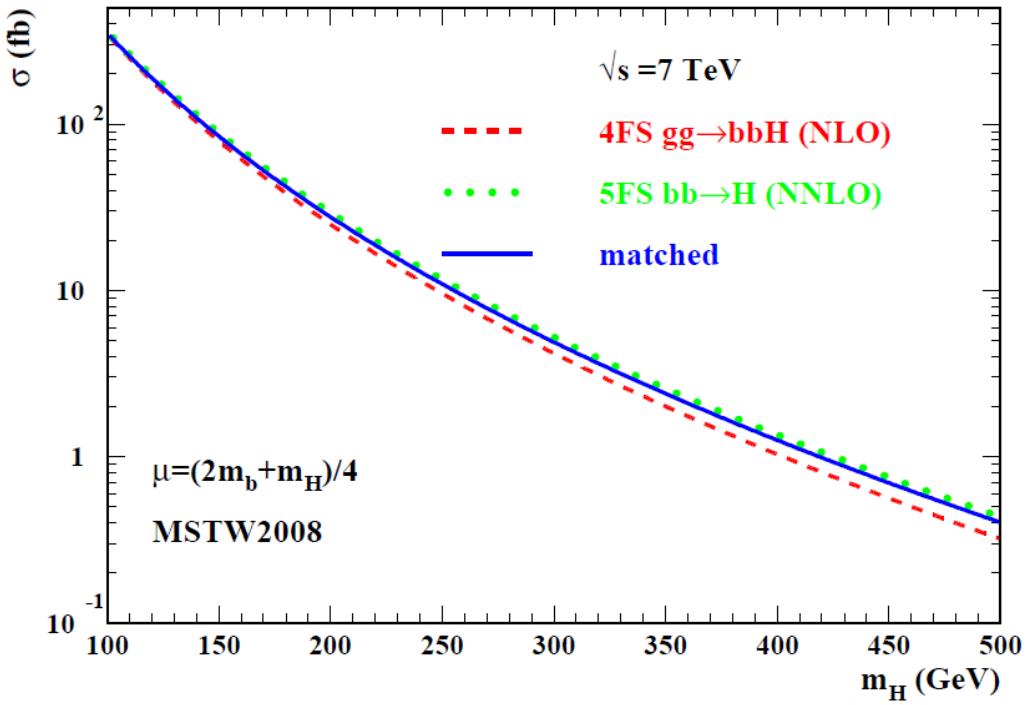

Charged Higgs(300 GeV) cross section

Expected cross section for H^+ production in association with a top quark (4FS and 5FS matched) times the branching fraction of $H^+ \rightarrow$ tb, as a function of (a) m_{H^+} in the m_h^{mod-} scenario and (b) tanβ for various MSSM scenarios

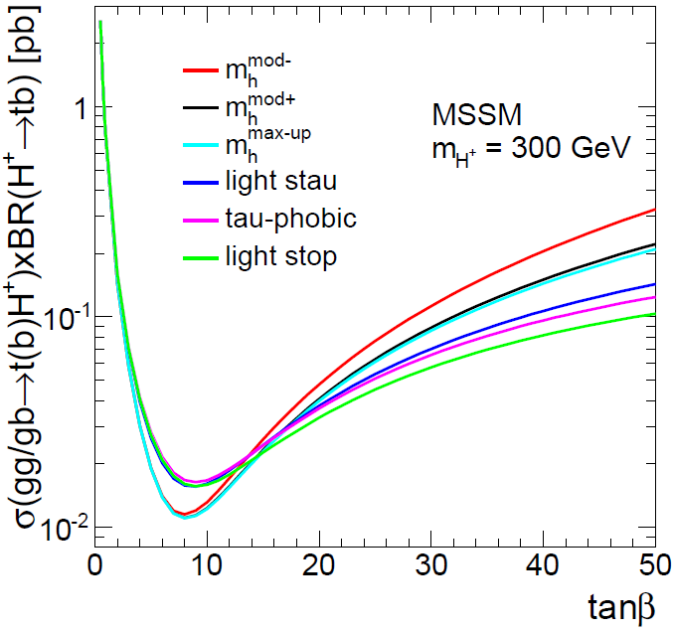

Charged Higgs(MSSM m_{hmod}) cross section

Expected cross section for H^+ production in association with a top quark (4FS and 5FS matched) times the branching fraction of $H^+ \rightarrow$ tb, as a function of (a) m_{H^+} in the m_h^{mod-} scenario and (b) tanβ for various MSSM scenarios

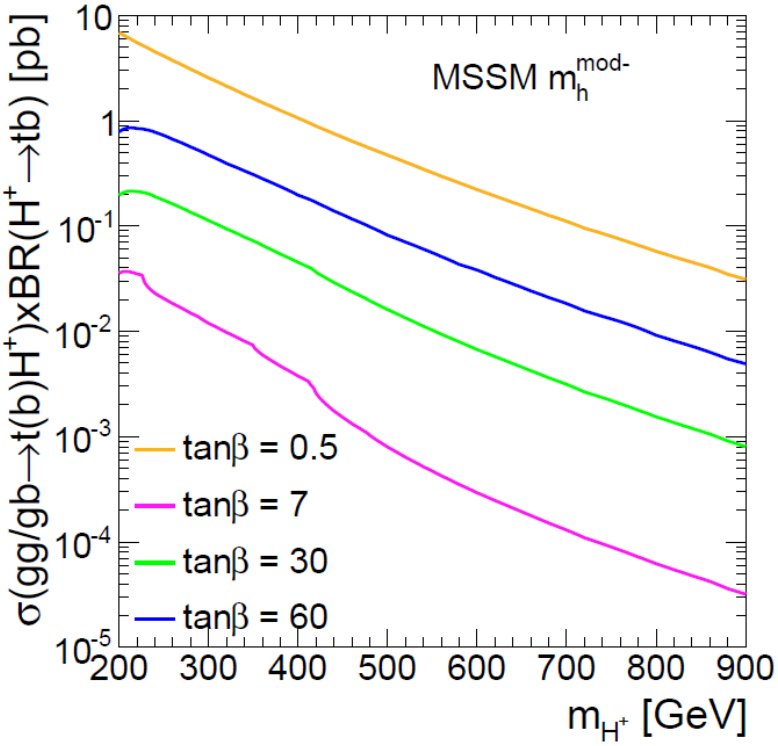

Expected cross sections m_h^{mod-} benchmark model of the MSSM

m_{H^+} [GeV]	200			400			600		
$\tan\beta$	0.5	0.7	0.9	0.5	0.7	0.9	0.5	0.7	0.9
$\sigma(gg/gb \to t(b)H^+)$ [pb]	6.86	3.50	2.11	1.07	0.55	0.33	0.23	0.12	0.072
BR($H^+ \to tb$) [%]	99.8	97.8	95.7	98.6	97.3	95.6	95.2	90.9	85.6
Γ_{H^+} [GeV]	4.19	2.18	1.34	64.9	33.6	20.7	114	61.2	39.3

Observed and expected 95% CL limits on $\sigma(gb \to tH^+) \times BR(H^+ \to tb)$

m_{H^+} [GeV]	Observed	Expected	-2σ	-1σ	1σ	2σ
200	6.28	3.78	2.03	2.73	5.23	7.05
225	3.83	2.40	1.29	1.73	3.33	4.55
250	4.20	1.98	1.06	1.43	2.76	3.81
275	2.78	1.69	0.91	1.22	2.34	3.18
300	2.89	1.44	0.77	1.04	2.00	2.75
350	1.57	0.96	0.52	0.69	1.34	1.83
400	1.04	0.64	0.35	0.46	0.90	1.23
450	0.91	0.45	0.24	0.32	0.64	0.88
500	0.68	0.40	0.22	0.29	0.57	0.79
550	0.51	0.31	0.17	0.23	0.45	0.64
600	0.24	0.25	0.13	0.18	0.36	0.51

Search and Limit: $H^{\pm} \rightarrow \tau^{\pm}\nu$

ATLAS-CONF-2014-050

- Hadronic τ channel
  - Low mass: 80 < $mH^{\pm}$ < 160 GeV for gluon fusion
  - High mass: 180 < $mH^{\pm}$ < 1000 GeV for with top quark
- Background (Data driven)
  - True τ: Embedding method
  - jet→τ: Mis identified lepton
- Background (MC)
  - e/μ→τ
- Upper limit on Br ($t \rightarrow bH^{\pm} \rightarrow Br(\tau\nu)$):
  1.3% ~ 0.23 %
  *previous: 2.1%~0.24%
- Upper limit:
  0.76 pb at 180 GeV
  4.5 fb at 1000 GeV
  *previous: 0.9~0.017pb

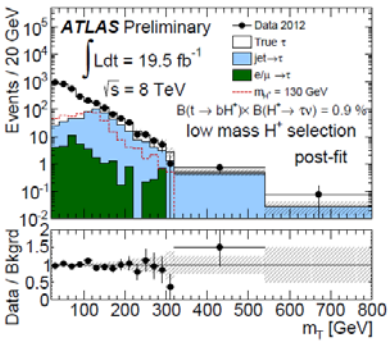

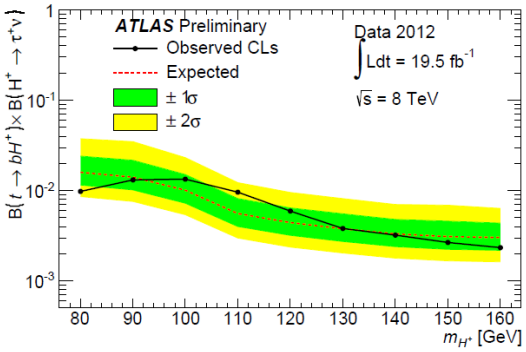

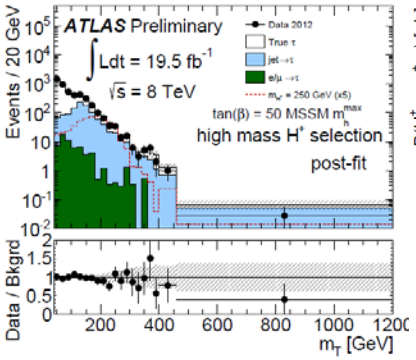

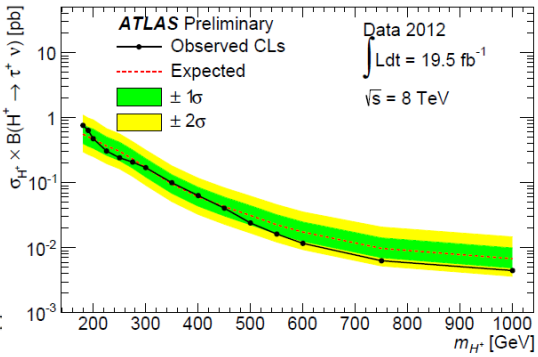

Exclusion plot for charged Higgs

Result from
$H^{\pm} \rightarrow \tau^{\pm}\nu$

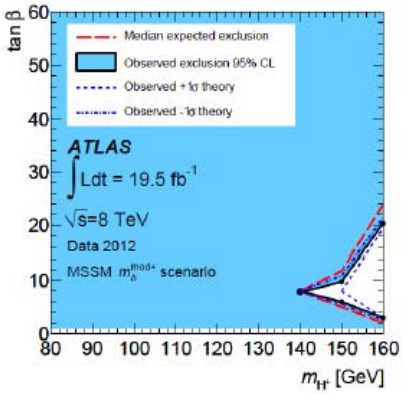

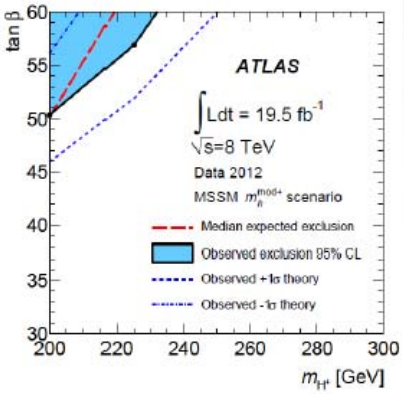

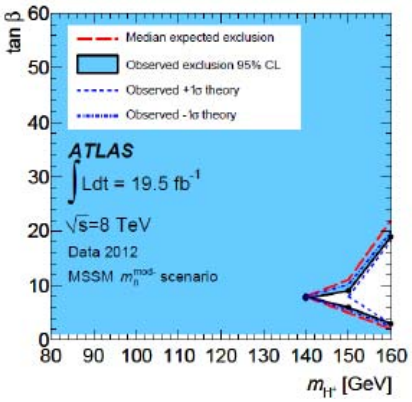

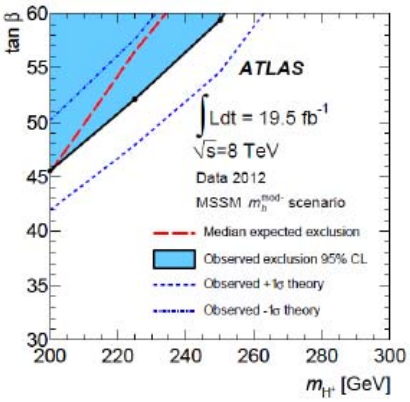

Search and Limit: $H^{\pm} \to \tau^{\pm}\nu$

CMS result

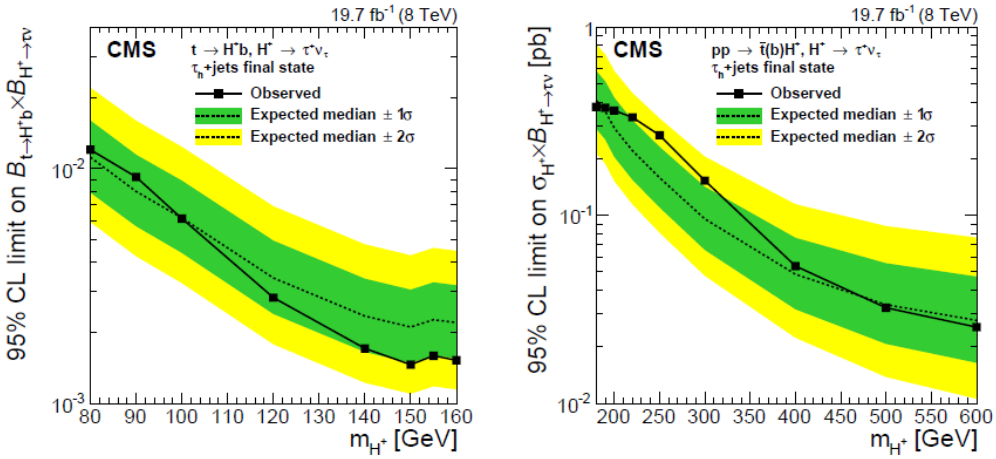

Figure 8: Expected and observed 95% CL model-independent upper limits on $\mathcal{B}(t \to H^+b)\,\mathcal{B}(H^+ \to \tau^+\nu_\tau)$ with $m_{H^+} = 80$–$160\,\text{GeV}$ (left), and on $\sigma(pp \to \bar{t}(b)H^+)\,\mathcal{B}(H^+ \to \tau^+\nu_\tau)$ with $m_{H^+} = 180$–$600\,\text{GeV}$ (right) for the $H^+ \to \tau^+\nu_\tau$ search in the τ_h+jets final state. The regions above the solid lines are excluded.

Cross section Limit: $H^{\pm} \to \tau^{\pm}\nu$

CMS result

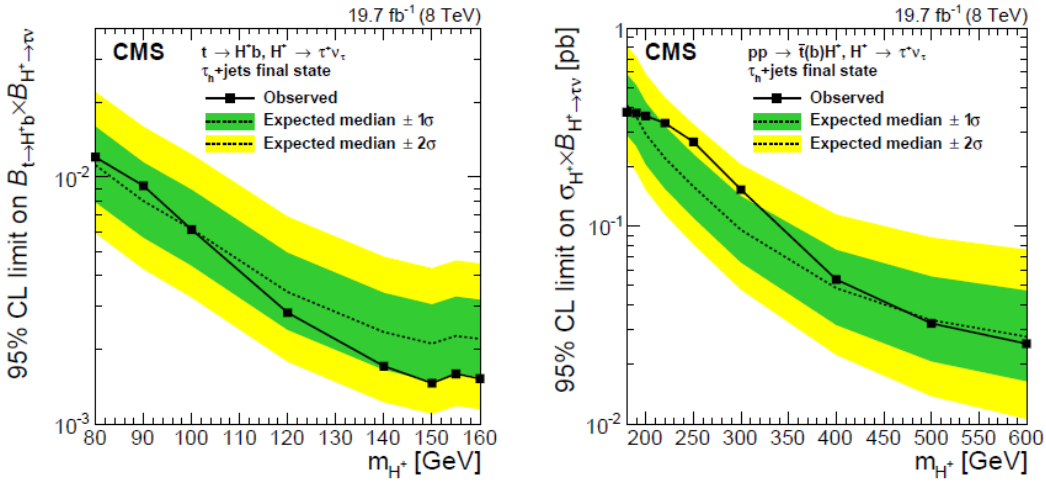

Figure 8: Expected and observed 95% CL model-independent upper limits on $\mathcal{B}(t \to H^+b)\,\mathcal{B}(H^+ \to \tau^+\nu_\tau)$ with $m_{H^+} = 80$–$160\,\text{GeV}$ (left), and on $\sigma(pp \to \bar{t}(b)H^+)\,\mathcal{B}(H^+ \to \tau^+\nu_\tau)$ with $m_{H^+} = 180$–$600\,\text{GeV}$ (right) for the $H^+ \to \tau^+\nu_\tau$ search in the τ_h+jets final state. The regions above the solid lines are excluded.

Cross section Limit: $H^{\pm} \rightarrow tb$

CMS result

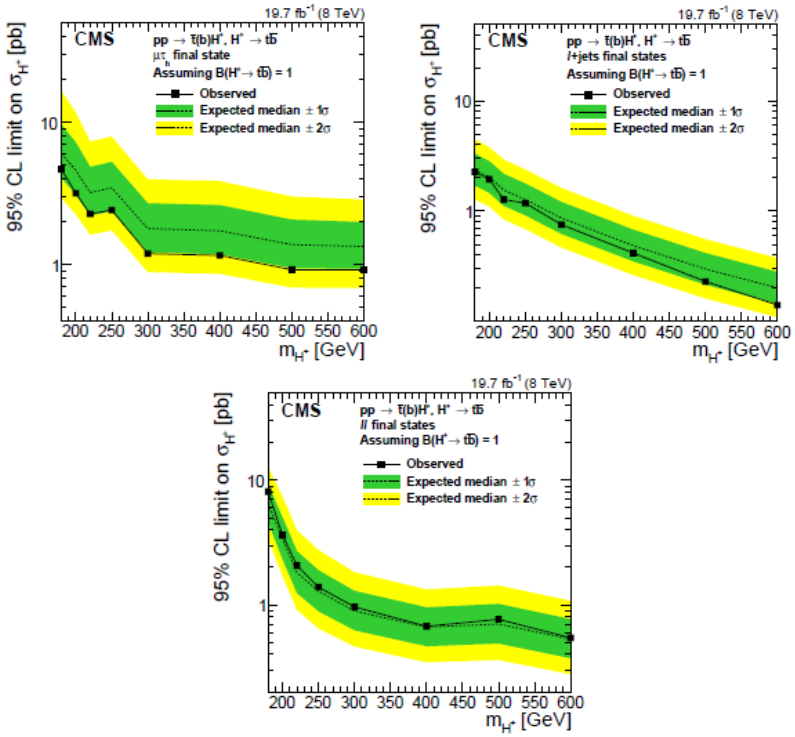

Figure 9: Expected and observed 95% CL upper limits on $\sigma(pp \rightarrow \bar{t}(b)H^+)$ for the $\mu\tau_h$ (upper left), ℓ+jets (upper right), and $\ell\ell'$ final states (bottom) assuming $\mathcal{B}(H^+ \rightarrow t\bar{b}) = 1$. The regions above the solid lines are excluded.

Cross section Limit: $H^{\pm} \rightarrow tb$

CMS combine result

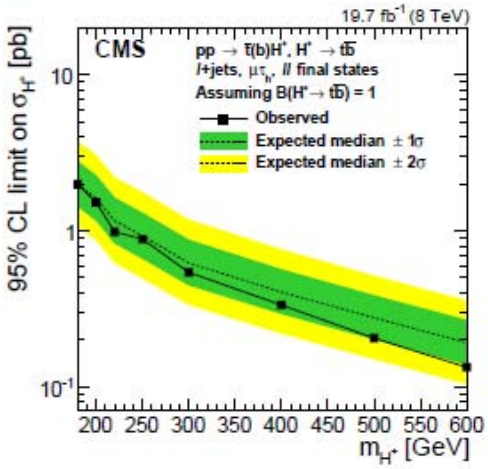

Figure 10: Expected and observed 95% CL upper limits on $\sigma(pp \rightarrow \bar{t}(b)H^+)$ for the combination of the $\mu\tau_h$, ℓ+jets, and $\ell\ell'$ final states assuming $\mathcal{B}(H^+ \rightarrow t\bar{b}) = 1$. The region above the solid line is excluded.

Exclusion reagion in mH⁺-tanβ plane: $H^{\pm} \rightarrow$ tb and $\tau^{\pm}\nu$

CMS combine result

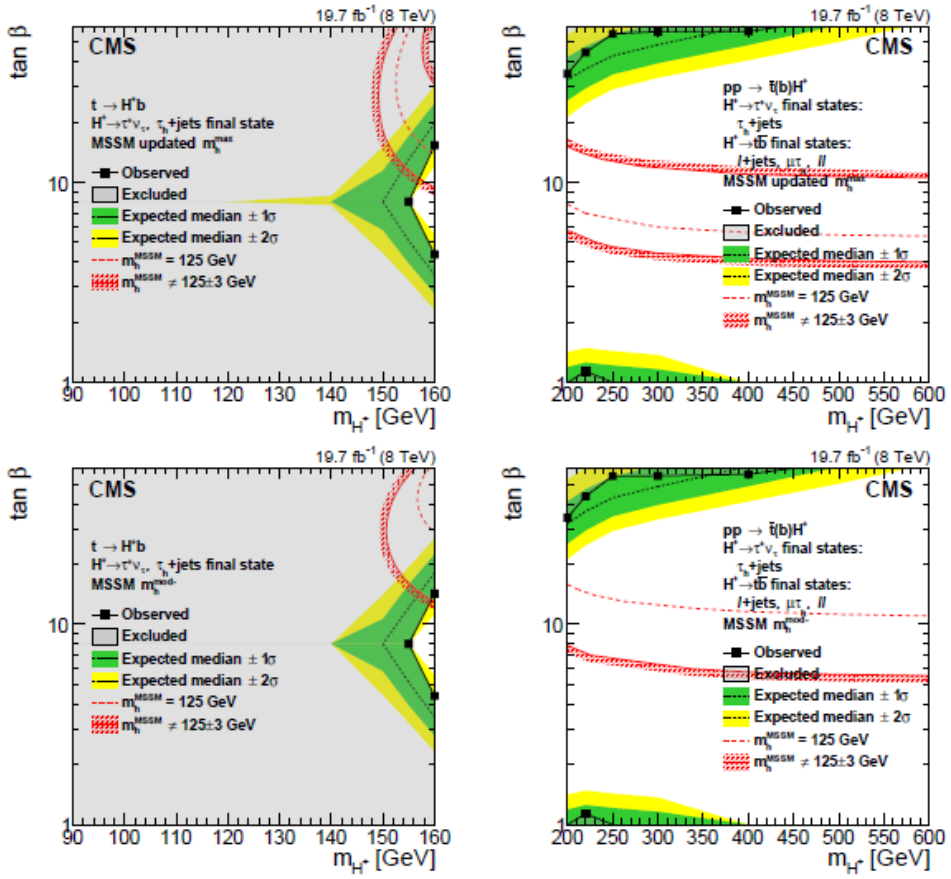

Text for exclusion reagion

CMS combine result

Figure 11: Exclusion region in the MSSM m_{H^+}–tan β parameter space for m_{H^+} = 80–160 GeV (left column) and for m_{H^+} = 180–600 GeV (right column) in the updated MSSM m_h^{max} scenario (top row) and m_h^{mod-} scenarios [29, 33] (bottom row). In the upper row plots the limit is derived from the $H^+ \rightarrow \tau^+\nu_\tau$ search with the τ_h+jets final state, and in the lower row plots the limit is derived from a combination of all the charged Higgs boson decay modes and final states considered. The $\pm 1\sigma$ and $\pm 2\sigma$ bands around the expected limit are also shown. The light-grey region is excluded. The red lines depict the allowed parameter space for the assumption that the discovered scalar boson is the lightest CP-even MSSM Higgs boson with a mass $m_h = 125 \pm 3$ GeV, where the uncertainty is the theoretical uncertainty in the Higgs boson mass calculation.

$H^{\pm} \rightarrow tb$ search in s-channel

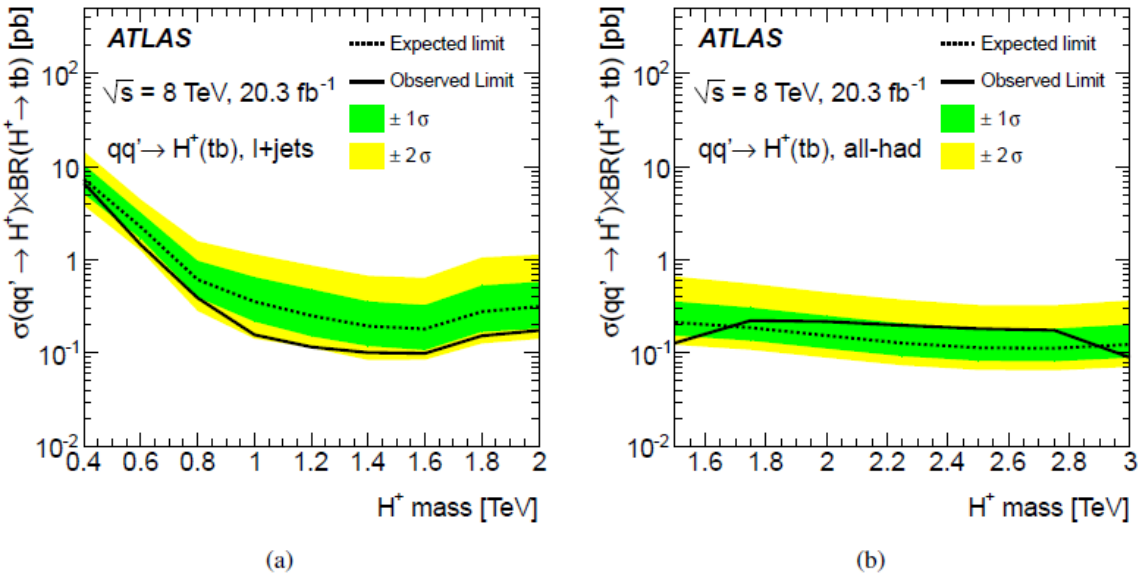

Figure 10: Expected and observed 95% CL limits on the *s*-channel production cross section times branching fraction for $H^+ \rightarrow tb$ as a function of the charged Higgs boson mass, in the (a) lepton+jets final state and (b) all-hadronic final state, including all systematic uncertainties, using a narrow-width approximation.

Luminosity ratio

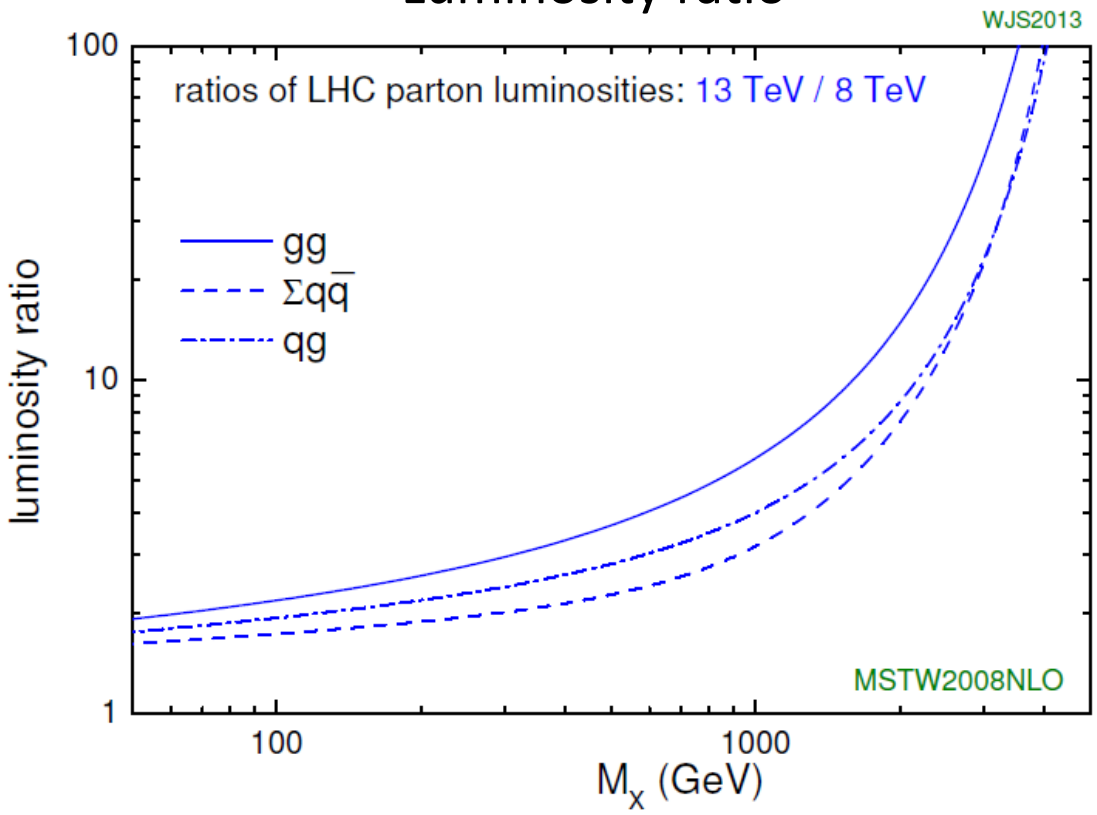

$\frac{Sens13TeV}{Sens8TeV} = \frac{\sigma sig13TeV \times \mathcal{L}sig13TeV}{\sigma sig8TeV \times \mathcal{L}sig8TeV} / \frac{\sqrt{\sigma bkg13TeV} \times \mathcal{L}sig13TeV}{\sqrt{bkg8TeV} \times \mathcal{L}bkg8TeV} =$ ~3/√3 ＊Lumiが同じ、かつ600GeV

ttbar cross section

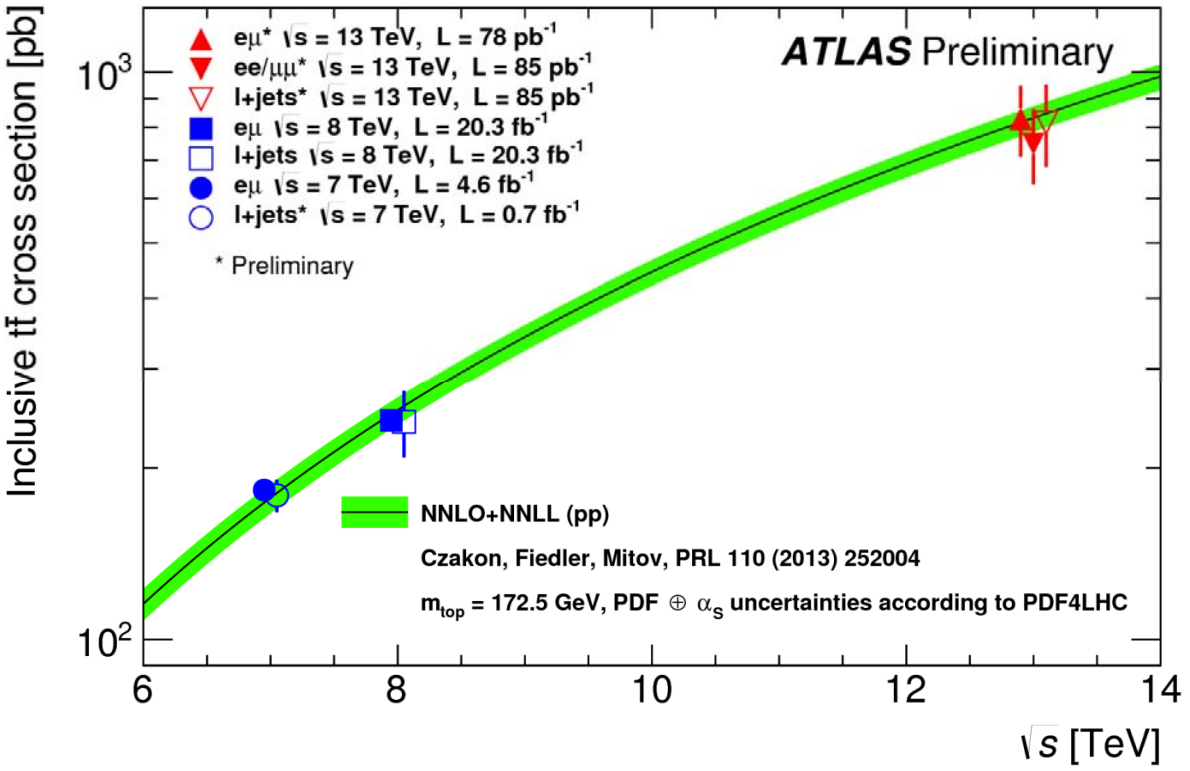

B-tag algorithm

- MV1 : multivariate tagging algorithm
  - IP3D: 主要崩壊点に対するtrackの衝突係数
  - SV1: 2次崩壊点
  - JetFitter: CハドロンやBハドロンの崩壊の幾何学的特徴